Optical-absorption bands in the 1–3 eV range in *n*-type SiC polytypes

Sukit Limpijumnong, Walter R. L. Lambrecht, Sergey N. Rashkeev, and Benjamin Segall
Department of Physics, Case Western Reserve University, Cleveland, Ohio 44106-7079
(Received 22 December 1998)

Measured optical-absorption bands in the 1–3 eV range in fairly heavily doped *n*-type SiC polytypes 3C, 6H, 4H, 8H, and 15R are shown to arise from optical transitions between the lowest conduction band, which is to some extent perturbed by impurity effects, to higher conduction bands. The energies of the transitions are in good agreement with the differences between unperturbed low-lying energy bands calculated using the full-potential linear muffin-tin orbital method in the local-density approximation. The polarization dependence is explained by selection rules deriving from the symmetry of the bands involved. This indicates that the states involved in the transitions must to a good extent retain the symmetry characters of the unperturbed bands. On the other hand, the calculated absorption peaks from a pure band-to-band model are much narrower, and slightly lower in energy than the experimental ones. Calculations of the density of states over a restricted range of **k** space for the final states indicate that a partial breakdown of periodicity and hence the $\Delta\mathbf{k}=0$ selection rule can account for a major part of the broadening. This explanation is consistent with the degenerate carrier concentration, associated with the overlap of the impurity band tail with the bottom of the conduction band. In 6H-SiC, one feature in the absorption spectrum appears nevertheless to be associated with a more purely band-to-band-like transition. It is a sharp one-dimensional van Hove singularity in the joint density of states at the *M* point associated with the camel's-back structure of the lowest conduction band. At a lower carrier concentration, this feature is not present, and the transitions appear to have a more localized impurity-to-band character. [S0163-1829(99)05420-X]

I. INTRODUCTION

Optical-absorption spectra in semiconductors are normally dominated by transitions from the valence to the conduction bands, but can also show relatively strong defect-related absorption bands below the fundamental gap. In silicon carbide (SiC) the gap, which is indirect in all known polytypes, ranges from 2.416 eV (in 3C) to 3.33 eV (in 2H). In *n*-type doped material with carrier concentrations in the range $10^{17}<n<10^{19}$ cm^{-3}, well-defined absorption ''bands'' were observed below the band in the 1–3-eV gap.[1–7] In addition, these samples typically (i.e., all the above references with the exception of Ref. 7) also show a Drude-like absorption at low energies (<1 eV). This indicates that these samples were degenerately *n* type, and consequently have a significant free-carrier absorption. It was thus suggested that these optical-absorption bands are associated with band-to-band transitions between the lowest conduction band and the higher-lying bands.[4]

One reason for the interest in these absorption bands is that they appear to be responsible for the color of the crystals. As explained by Patrick and Choyke,[5] the dominant absorption in platelet-like (noncubic so-called α-SiC) crystals occurs for the $\mathbf{E}\perp\mathbf{c}$ polarization. While pure α-SiC crystals only absorb in the UV, and are therefore transparent, the extra absorption band just below 3 eV in the blue region can explain the yellow appearance in *n*-type 15R. The additional absorption band in the 6H polytype peaks at 2 eV (in the orange) and leads to a greenish color. In 3C-SiC, the weak intrinsic absorption in the blue is responsible for a yellowish color in relatively pure crystals. It shifts somewhat toward the green by additional free-carrier absorption in the red region. Additional absorption bands which will be seen to occur for $\mathbf{E}\|\mathbf{c}$ in *n*-type doped samples are much stronger, but have little effect on the color of platelet crystals.

While the earliest observation[1] of these 1–3-eV specific absorption bands was restricted to $\mathbf{E}\perp\mathbf{c}$ and to ''hexagonal'' or α-SiC, i.e., without full determination of the actual polytype, the work of Biedermann[4] showed distinct spectra for $\mathbf{E}\perp\mathbf{c}$ and $\mathbf{E}\|\mathbf{c}$ polarizations, and clear differences between the 6H, 4H, 8H, and 15R polytypes. Ellis and Moss[3] observed the polarization dependence for 6H-SiC slightly earlier. Violina, Liang-hsiu, and Kholuyanov,[2] and later Dubrovskii and Radovanova,[6] studied the temperature dependence of these spectra in 6H-SiC, and simultaneously studied the free-carrier concentrations by means of Hall measurements while Biedermann's work gives only an estimate of the carrier concentration. The authors of Ref. 2 also observed an extra peak just above 1 eV, in samples of relatively low carrier concentration (4×10^{18} cm^{-3}), which appears to be buried under the free carrier absorption in other studies. Patrick and Choyke[5] found a single ''extra'' absorption band in *n*-type 3C-SiC, and studied its temperature dependence.

The correlation of the intensities of these absorption bands with carrier concentration as determined by Hall measurements, and the simultaneous changes in the free-carrier absorptions, provide strong evidence in favor of the band-to-band interpretation. The narrowing and small shift of the spectra upon cooling were observed by Patrick and Choyke to be similar to those known for Ge inter-valence-band transitions. Nevertheless, Patrick and Choyke[5] cautioned that because the interband absorption shape was not well known at the time of their work, that observation could not answer the question of whether the initial state of these transitions were defect level-like or bandlike. Dubrovskii and Radovanova[6] argued on the basis of their observation of a shift of the

spectra with temperature that there is a crossover from a band-to-band transition to a defect-to-band transition mechanism as one lowers the temperature. On the basis of measurements on a relatively weakly *n*-type doped 6H sample, Stiasny and Helbig[7] concluded that the absorption bands being considered are in fact due to transitions between states of a deep center and not to the mechanism assumed here. A discussion of their data and their analysis will be presented below.

The present status of first-principles band-structure calculations makes it possible to analyze the origin and nature of these spectra in more detail than was possible at the time of the experimental studies referred to above. In particular, we now have the opportunity to determine the validity of the interpretation of these spectra as band-to-band transitions by a careful comparison of the calculated interband separations and the polarization dependences for the different polytypes with the data. That was our original goal. At the same time, we hoped this exercise would provide a test of the accuracy of our earlier first-principles band-structure results.[8–10] We indeed find that the band-structure energy differences and band symmetries account well for the observed absorption bands and their polarization. While some preliminary results were presented in a conference proceedings,[11] we provide a full account of this study in the present paper. We show that our analysis applies to all the polytypes studied in Biedermann's paper (6H, 4H, 15R, and 8H) and to 3C-SiC,[5] and accounts well for the polytype dependence of the spectra.

However, when the absorption coefficients associated with transitions between the unperturbed bands were calculated, it became evident that significant discrepancies exist between the peak widths of the measured and calculated spectra.[11] It is reasonable to infer that this is due to the effects associated with the heavy doping. With carrier concentrations of order 10^{19} cm^{-3}, the shallow nitrogen defect levels must significantly broaden into a band which overlaps with the bottom of the conduction band, forming a so-called band tail. Thus this problem relates directly to the question raised above about whether the initial states are defectlike or bandlike. We show here that the broadening can mainly be explained by a partial breakdown of the ''vertical,'' $\Delta\mathbf{k}=0$, selection rule associated with the fact that the lowest conduction band, which provides the initial states of the transitions, is significantly ''perturbed'' by the impurities. Perturbed in the present context means that the center of gravity of the initial states is slightly shifted towards lower energies, i.e., into the band tail, and that the above selection rule must be relaxed as a result of the breakdown of perfect crystalline periodicity. We show this by calculating densities of states (DOS) of the higher bands over an appropriately limited range of **k** space associated with the transitions from the initial states.

At the same time, a particular feature in 6H-SiC still appears to be associated with a particular ''pure'' band-to-band transition because it is strongly enhanced by the occurrence of a van Hove singularity. That feature is closely related to the occurrence of a camel's-back structure of the lowest conduction band, which we found in earlier work to have a minimum along ML and a saddle point at M. This structure was earlier predicted to have an impact on optically detected cyclotron resonance spectra,[12] but still requires definitive experimental confirmation.[13] We propose that a further experimental investigation of the presently discussed absorption spectra may provide further evidence for the occurrence of this saddle point.

Apart from this singularity in 6H, our analysis indicates that most of these optical transitions have a mixed ''impurity level-to-band'' and ''band-to-band'' nature, reflected, for example, in the fact that they obey the selection rules expected from the symmetry character of the bands, but nevertheless are affected significantly by the impurity effects in their *k*-selection rule. For much lower carrier concentrations, transitions of a slightly more localized level-to-band nature appear to be able to explain the spectrum observed by Stiasny and Helbig.[7]

The rest of the paper is organized as follows. We first provide some details on our computational approach for the band structures, and describe how the optical absorption is calculated in Sec. II. In particular, we describe our approach to mimic the impurity effects by calculating a density of final states sampled over a limited region of **k** space. Next, in Sec. III, we present our results in subsections organized per polytype. For each polytype, we show the experimental spectra along with calculated spectra of the absorption coefficient $\alpha(\omega)$ calculated assuming strict adherence to the $\Delta\mathbf{k}=0$ selection rule, and, in addition show our partial **k**-space DOS. The first allows us to assess the polarization dependence, the second the width and peak positions. Finally, we summarize the conclusions of our work.

II. THEORETICAL MODEL

As already mentioned in Sec. I, it is clear that when the carrier concentration is as high as 10^{19} cm^{-3}, as is the case in most of the samples under consideration, the use of an unperturbed band model is questionable. The shallow nitrogen levels which are associated with the *n*-type doping at these concentrations must form an impurity band of significant width. The N impurity in SiC polytypes is known to lead to several shallow levels depending on the site it occupies, and depending on the polytype.[14] In particular, N at the hexagonal (h) sites have typically a lower binding energy than those at cubic (k) sites. In 4H-SiC, the h level has been determined to be 45 and 52 meV by Hall and IR-absorption measurements, respectively. Similarly, the k level is found at 100 and 91 meV. In 6H, the h level is located at 81 and 100 meV (depending on the technique), and the two different k levels at a 125–150 meV according to Hall and 137–142 meV according to IR absorption. In 3C-SiC, the N donor level is thought to be at 48–55 meV. As one can see, there are differences of the order of 50 meV between the binding energies at different sites. Due to the random potential fluctuations at high concentration and the overlap of the donor wave functions, it is plausible that at least the most shallow of these levels exhibit broadening to the extent that they overlap with the bottom of the lowest conduction band, and hence lead to an exponential band tailing associated with a degenerate carrier concentration (even at room temperature). Evidence for this comes, for example, from Hall measurements in 3C-SiC with varying concentrations of donors,[15] which indicate that the ''effective'' donor binding energy $E_d(N_d)$ based on a one-band model goes to zero as $E_d(N_d)$

$=E_d(0)-\alpha N_d^{1/3}$, with $\alpha \approx 2.6\times 10^{-5}$ meV cm and $E_d(0) \approx 48$ meV, at donor concentrations of about 6×10^{18} cm^{-3}. One should also keep in mind that if there is compensation by acceptors (as is likely), a carrier concentration of $n = 10^{19}$ cm^{-3} implies an even higher concentration of donor levels. Thus our basic model is that there is a continuous and exponentially decreasing distribution of shallow donor levels extending down to about 0.1 eV below the band. The states in this distribution become more localized as the energy lies further below the band edge. Nevertheless, since all of these states can be thought of as being derived from the lowest conduction-band state as the envelope function, one might expect that these states would still reflect the symmetry character of the lowest conduction band. In this context, it is important to point out that the effective-mass approximation restricted to the lowest conduction band provides a fairly good model for the N donor levels when central cell and multiple valley effects are taken into account.[16] This approximation starts to break down for the deeper levels, such as the *k*-site level in 6H. Possibly, this deeper level at the cubic sites in 6H may remain a separate level as opposed to being part of the band tail.

Unfortunately, a direct treatment of the system as described above including the defect levels explicitly is not feasible. Thus we will attempt first to model the interconduction-band transitions based on an unperturbed band-structure model. In that model, it is assumed that for a given donor concentration, the lowest band is filled up to some level according to the density of states and the Fermi function, i.e., the Fermi level E_F is determined from

$$n=\int_{E_c}^{E_F} N_c(E)\,dE, \tag{1}$$

in which E_c is the conduction-band minimum, $N_c(E)$ the DOS in the conduction band, and n the total number of carriers. The transitions to the higher levels are then calculated assuming that they are ''vertical'' ($\Delta\mathbf{k}=0$). Specifically, we calculate the imaginary part of the dielectric function

$$\epsilon_2^j(\omega,T)=\frac{e^2}{m^2\omega^2\Omega\pi}\sum_{if}\sum_{\mathbf{k}}[f_{i\mathbf{k}}(T)-f_{f\mathbf{k}}(T)]|\langle i\mathbf{k}|p^j|f\mathbf{k}\rangle|^2\delta(E_{f\mathbf{k}}-E_{i\mathbf{k}}-\hbar\omega), \tag{2}$$

where $E_{n\mathbf{k}}$, with $n=i$ and f for initial and final states, are the band energies, which we take to be independent of temperature; p^j is the jth Cartesian component of the momentum operator, $f_{n\mathbf{k}}(T)=[1+\exp(E_n-E_F)/kT]^{-1}$ are Fermi factors; Ω is the unit-cell volume; and e and m are the electronic charge and mass. In practice, the summation over $\mathbf{k}$ is restricted to a small region near the minimum of the lowest conduction band i. From it, we obtain the absorption as

$$\alpha(\omega)\approx\omega\epsilon_2(\omega)/n_0c, \tag{3}$$

where n_0 is the low-frequency index of refraction, the frequency dependence of which is neglected over the range of interest for simplicity.

These calculations are performed using the energy bands obtained from a full-potential linear muffin-tin orbital (FP-LMTO) calculations. The matrix elements, however, were calculated in the atomic sphere approximation (ASA).[17] In previous calculations of linear[10,18] and nonlinear optical response[19] for SiC, we have shown that the ASA generally provides quite adequate band structures and matrix elements.[20] However, since some details of the band structure are important here, we prefer to employ FP-LMTO bands. This leads, for example, to a reversal in the ordering of the two lowest conduction bands at M in 4H which are less than 100 meV apart.[13]

The version of the FP-LMTO method used here was developed by Methfessel.[21] The self-consistent potential used in this method is based on the local-density approximation for exchange and correlation[22] within the density-functional theory.[23]

Next we attempt to mimic at least one important effect of the defect perturbations on the transitions, namely, the breakdown of the $\Delta\mathbf{k}=0$ selection rule. As noted in Sec. I, under the heavy doping in the samples considered, the conduction-band states are expected to merge with the N impurity band levels. Consequently, the density of initial states should be significant down to the energies around the shallow N donor level. It is then reasonable to assume that the extent of the localized states therein is characterized by the radius R of the donor state, given by effective-mass theory to be $\sim$20–25 Å . The corresponding spread in k, $\propto R^{-1}$, is then approximately given by $\delta k\approx 0.1(2\pi/a)$, with a the lattice constant. A similar estimate is obtained by considering that the random part of the potential due to the impurities must have a length scale corresponding to the average distance L between impurities. For $N_d=10^{19}$ cm^{-3}, one finds that $L\approx N_d^{-1/3}$ must be of the order of 5 nm. Thus we calculate densities of states in the conduction band within a sphere of this size δk around the k point at which the minimum of the lowest conduction band lies. In 6H, where the lowest band is very flat, the broadening in energy originating from the initial state's k spread is negligible compared to that resulting from the spread in $\mathbf{k}$ of the final states. We perform these calculations band by band, so that we can examine their separate band-by-band contributions. The matrix elements turn out to exhibit rather weak dependences on $\mathbf{k}$ in the region of interest and thus can be taken as a constant for each pair of bands ($\bar{M}_{if}^j$). Within such an approximation, the absorption curve could be modeled as

$$\alpha^j(\omega)\propto\sum_{if}|\bar{M}_{if}^j|^2N_f(E_i+\hbar\omega)N_i(E_i), \tag{4}$$

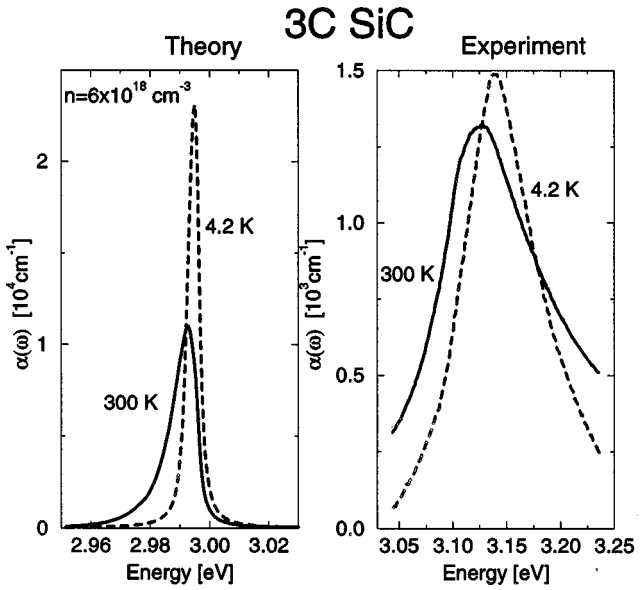

FIG. 1. Calculated inter-conduction-band spectrum in 3C-SiC at high and low temperatures compared to the experimental data of Ref. 5. The carrier concentration in the theory was chosen so as to make the area under the curve approximately equal to that in the experiment.

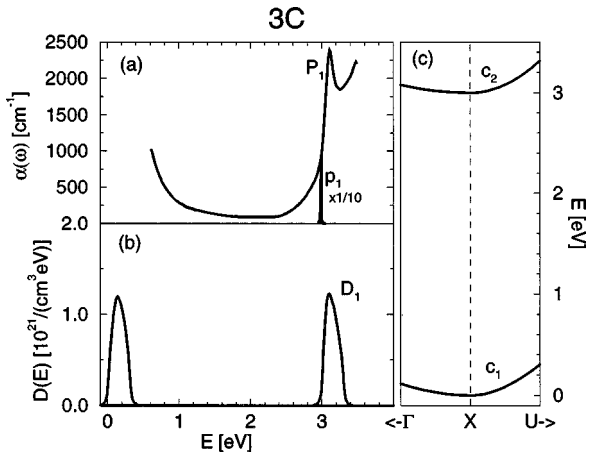

FIG. 2. Band structure and inter-conduction-band spectrum in *n*-type 3C-SiC: (a) Experimental absorption spectrum from Ref. 5 at 300 K with the peak P_1 compared to the peak p_1 calculated in the pure band-to-band limit with $n=6\times10^{18}$ cm^{-3}. (b) Calculated density of states within $\delta k=0.1$ $[2\pi/a]$ from $\mathbf{k}_{min}=X$. (c) Energy bands around X.

where, as before, j defines the polarization. In other words, we now have essentially a convolution of the density of initial $N_i(E)$ with the density of final states $N_f(E)$, and where the density of initial states is assumed to run over the band-tail distribution and the density of final states is calculated within the range δk described above. We will not attempt to construct $\alpha(\omega)$ functions explicitly in this manner because of the various uncertainties associated with the tail distribution function. Nevertheless, this expression suggests that one can essentially take the $\alpha(\omega)$ functions to be a sum of the restricted k-region densities of states multiplied by the matrix element weight factor appropriate to the pair of bands occurring in the original pure band-to-band model, and with perhaps some additional asymmetric broadening due to the distribution of initial states in the band tail. This should be sufficient to correlate the calculated quantities here, and shown in Sec. III with the experimental spectra.

III. RESULTS

A. 3C

In 3C-SiC, three equivalent minima of the conduction band lie at the ends of the $\langle 001\rangle$ axes. Each minimum is a X_{1c} state and the next level is a X_{3c} state 3.0 eV above it. Because of cubic symmetry, the $\alpha(\omega)$ tensor is isotropic.

The right-hand panel of Fig. 1 shows the inter-conduction-band absorption data obtained by Patrick and Choyke[5] after subtraction of the background intrinsic indirect absorption (see Fig. 2). The left-hand panel displays the calculated absorption for the two temperatures used in the experiment and for a carrier concentration of $n=6\times10^{18}$ cm^{-3}, which gives the area under the peak equal to that in the experiment. Note the difference in scales. Patrick and Choyke suggested that the carrier concentration in their sample was indeed of the order of 10^{19} cm^{-3}. We note that the theoretical peak occurs about 0.1 eV below the experimental peak and that the experimental peak is about a factor of 10 wider. A discrepancy by 0.1 eV in the interband separation of the X_{3c} and X_{1c} state could be due to the different quasiparticle corrections to the local-density-approximation eigenvalues for these states. The currently available GW calculations[24–26] indeed indicate a slightly larger shift for the X_{3c} state than for the X_{1c} state by about 0.1–0.2 eV. We note however, that this is within the current error bar of GW calculations. Generally speaking current GW calculations tend to find larger shifts for levels at higher energies, while this trend is not clearly supported by experiment.[18] A likely contribution to this 0.1-eV difference is the fact that some of the initial states lie in the band tail below the conduction-band edge. In any case, a discrepancy by only 0.1 eV in peak position is to be considered good agreement.

The width is clearly a more serious problem and is one of the main issues of this paper. To address it we refer to Fig. 2. Panel (a) shows the full measured absorption coefficient at 300 K in the 0–3.5-eV range, as well as the calculated interband absorption assuming unperturbed bands and vertical transitions. The experimental and calculated interband absorptions are labeled P_1 and p_1, respectively (and were given in more detail in Fig. 1). Panel (c) displays the unperturbed energy bands around the conduction-band minimum point X. In line with the discussion at the end of Sec. II, panel (b) shows the DOS for the two relevant conduction bands within the restricted k-space region of radius $0.1(2\pi/a)$ around X. It is evident that the width of D_1 is comparable to that of the measured peak P_1. One may also note that D_1 is shifted slightly upwards from p_1. This results simply from the fact that the relaxation of the $\Delta\mathbf{k}=0$ rule allows for transitions to higher energy. The peak maximum results from the cutoff of the k-space region included. An additional shift expected from the lowering of the initial states below the band is not included in this calculation.

Returning for a moment to Fig. 1, one may note that the experiment shows a shift of about 13 meV toward lower energies at room temperature compared to 4.2 K. This results

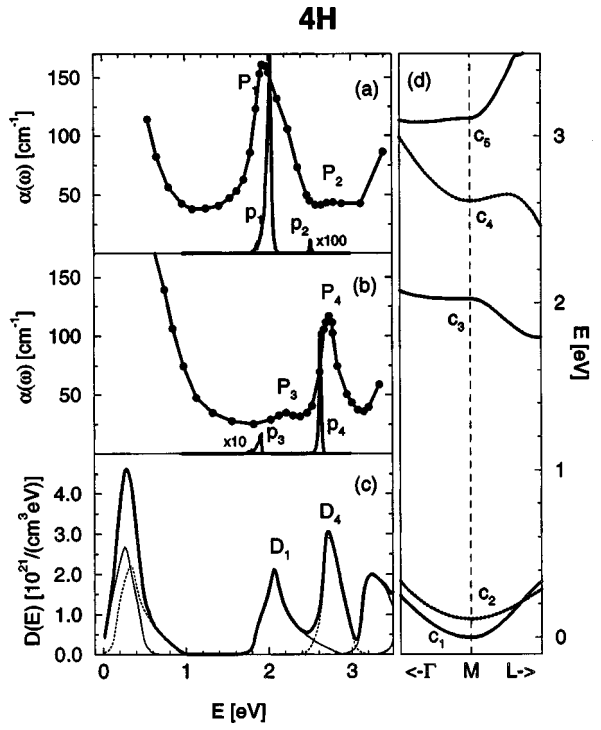

FIG. 3. Band structure and inter-conduction-band spectra in *n*-type 4H-SiC: (a) $\mathbf{E}\|\mathbf{c}$ and (b) $\mathbf{E}\perp\mathbf{c}$ experimental absorption spectra from Ref. 4 (lines connecting dots) with capitalized peak labels P_i compared to calculated spectrum in pure band-to-band limit (full line) peaks labeled by lower case p_i (assuming $n=10^{19}$ cm^{-3} and $T=300$ K). (c) Calculated density of states within $\delta k=0.1\ [2\pi/a]$ from $\mathbf{k}_{min}=M$. Thick line: total; full thin line: M_1 symmetry bands; dashed line: M_3 symmetry. (d) Energy bands: full lines correspond to M_1 symmetry and dashed lines to M_3 symmetry at *M*.

in part from the difference in the hydrostatic deformation potentials between X_{1c} and X_{3c} states, which accounts for about 4 meV (using a thermal expansion coefficient of 2.77×10^{-6} K^{-1} and a deformation potential difference $d[E(X_{3c})-E(X_{1c})]/d\ln\Omega$ of 4.3 eV (Ref. 27)), and in part from phonon effects on these states. The theoretical curves presented do not include these shifts, but do include a minor shift resulting from the finite temperature Fermi function.

B. 4H

Our results for 4H-SiC are shown in Fig. 3, which is organized similarly to Fig. 1, except that now we have to include the polarization dependence. In the right-hand panel (d), we show the energy bands of interest near the conduction band minimum at *M*. They are labeled c_1–c_5 in order of increasing energy at *M*. Their symmetry character, following the notations of Rashba,[28] is indicated as follows: full lines correspond to M_1 symmetry at *M* and U_1 along *ML*, while dashed lines correspond to M_3 (or U_3). To clarify the meaning of these labels, we recall that the space group is C_{6v}^4. The symmetry of the states at *M* are determined by the point group of the **k** vector at *M*, which is C_{2v}. It includes the rotation or reflection components of the space group operations, which leave *M* invariant. These are a mirror plane σ_1 passing through the Γ-*M* line, a glide mirror plane σ_1' normal to it passing through Γ-*K*, and a twofold rotation screw axis. The M_1 representation is fully symmetric with respect to all these operations, while the M_3 operation is antisymmetric with respect to the latter two operations and symmetric with respect to the former. These are the only two symmetries occurring for the bands of interest. From simple symmetry considerations, it can be shown that $\mathbf{E}\|\mathbf{c}$ transitions are allowed only between bands of the same symmetry, while, for $\mathbf{E}\perp\mathbf{c}$, transitions are allowed between M_1 and M_3 but forbidden between bands of the same symmetry.

For the carrier concentrations ($n\approx10^{19}$ cm^{-3} involved here and for temperatures not far above room temperature) only the lowest conduction band contains a sufficient number of electrons to contribute to the absorption. Hence we can limit our attention to transitions with the M_1 state as the initial state. Thus we expect mainly a peak at 2.0 eV arising from the $c_1\rightarrow c_3$ transition for $\mathbf{E}\|\mathbf{c}$, and a peak at 2.3 eV for $\mathbf{E}\perp\mathbf{c}$ corresponding to the $c_1\rightarrow c_4$ transition. Transitions to band 5 are also allowed for $\mathbf{E}\|\mathbf{c}$, but already start to overlap with the indirect valence to conduction band transitions.

In panels (a) and (b), the lines connecting the dots reproduce the experimental data of Ref. 4. We note that for each of the polarizations they indeed have their main peaks close to the above-mentioned energies. However, slight shifts in peak position and a large discrepancy in peak widths are apparent when the calculated $\alpha(\omega)$ based on the unperturbed band-to-band model are compared with the experimental spectra. The former was calculated for $T=300$ K, and thus also includes a slight occupation of the second conduction band, resulting in peaks labeled p_2 and p_3. Traces of these are recognizable in the experiment.

Panel (c) shows the DOS calculated with a radius $\delta k=0.1\ [2\pi/a]$ around the *M* point. The heavy line shows the total DOS, the full thin line shows the partial DOS corresponding to bands of symmetry M_1, and the dashed thin line the partial DOS corresponding to bands of symmetry M_3. Clearly, the width of peak D_1 corresponding to band c_3 is now comparable with the experimental width of peak P_1. There is a slight difference of 0.1 eV between the positions of D_1 and P_1. As for the case of 3C-SiC, this may in part reflect a slightly higher quasiparticle shift of band c_3 compared to band c_1, but it may also in part reflect the fact that the initial states of the transition are centered slightly below the band edge because of the mixing with the impurity band.

We note that relaxing the $\Delta\mathbf{k}=0$ rule not only has the effect of broadening the peaks but also of slightly shifting the peak maximum. D_1 peaks slightly above p_1 and D_4 peaks slightly above p_4. In fact, the peak positions of D_4 and P_4 appear to be in better agreement than those of D_1 and P_1. This might indicate that slight differences in quasiparticle correction apply to bands c_3 and c_4. As these differences are of order 0.1 eV, however, they are within the precision of current *GW* calculations. On the other hand, the slightly larger width of peak P_1 than that of P_4, as well as the asymmetry of these peaks, appears to be well reproduced by the shapes of D_1 and D_4. This supports the validity of our model, which was described in Sec. II.

Because the carrier concentration for the samples in Biedermann's paper[4] were given only roughly, it is not worthwhile to attempt to calculate and compare absolute intensities. As far as relative intensities are concerned, we note that this is also complicated by the need for including nonvertical

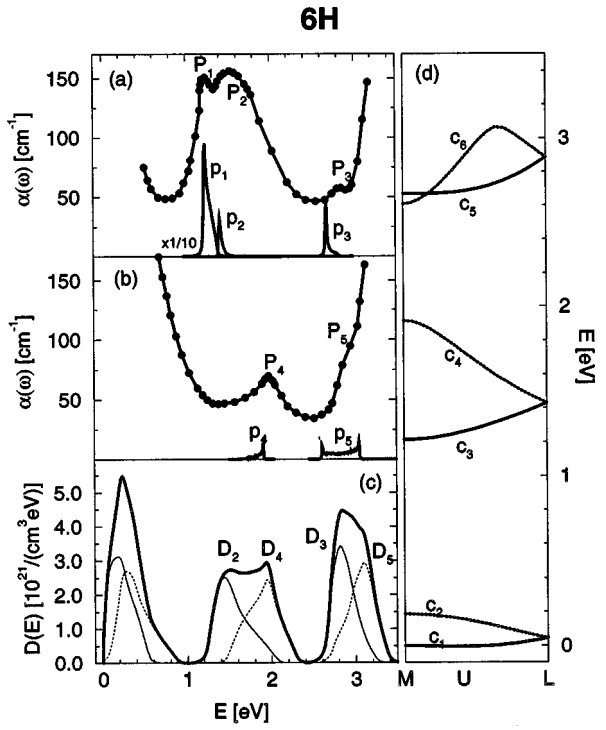

FIG. 4. Band structure and inter-conduction-band spectra in *n*-type 6H-SiC: (a) $\mathbf{E}\|\mathbf{c}$ and (b) $\mathbf{E}\perp\mathbf{c}$ experimental absorption spectra from Ref. 4 (lines connecting dots) with capitalized peak labels P_i compared to calculated spectrum in pure band-to-band limit (full line) peaks labeled by lower case p_i (assuming $n=10^{19}$ cm^{-3} and $T=300$ K). (c) Calculated density of states within $\delta k=0.1$ $[2\pi/a]$ from $\mathbf{k}_{min}=0.4\,ML$. Thick line: total; full thin line: U_1 symmetry bands; dashed line: U_3 symmetry. (d) Energy bands: full lines correspond to U_1 symmetry, and dashed lines to U_3 symmetry at $U=ML$.

transitions and the effects of the impurities. However, focusing on the two main transitions, we observe that the DOS peaks D_2 and D_4 appear to have similar intensities while the integrated absorption for P_1 is a few times larger than that for P_4. This is consistent with the fact that we find the matrix element for the allowed $c_1\rightarrow c_3$ transition to be about 2.5 times stronger than the $c_1\rightarrow c_4$ transition.

C. 6H

Our results for 6H-SiC are given in Fig. 4, which is organized in the same way as for 4H-SiC, except that now we display the energy bands in panel (d) along the entire ML line. This is done because band c_1 is extremely flat and has its minimum at about 0.4 ML. An enlargement of the dispersion along ML of the lowest band is shown in Fig. 5.

We note that the expected transitions for $\mathbf{E}\|\mathbf{c}$ are $c_1\rightarrow c_3$ and $c_1\rightarrow c_5$ and for $\mathbf{E}\perp\mathbf{c}$ are $c_1\rightarrow c_4$, $c_1\rightarrow c_6$. These transitions correspond, respectively, to P_1-P_2 (initially considered as a single feature) and P_3, and to P_4 and P_5. We note again the substantial underestimate of the peak widths in the pure band-to-band model (peaks labeled with lower case p_i). We note that p_1 was scaled down by a factor $\frac{1}{10}$ to fit into the frame of the figure, and is thus significantly stronger than the other p_i. The weak peak p_2 is due to the transitions $c_2\rightarrow c_4$ which requires the thermal occupancy of c_2. It does not significantly contribute to P_2, which is the strongest peak in the spectrum. The positions and widths of the partial **k**-space DOS D_2, D_3, and D_4 agree well with, respectively, P_2, P_3, and P_4, although P_3 is relatively weak because of the matrix element. To some extent D_4 also seems to contribute to the high-energy tail of P_2. This indicates a partial breakdown of the symmetry selection rules as well as the $\Delta\mathbf{k}=0$ selection rule. The exact experimental location of P_5 is difficult to extract because of its proximity to and overlap with the indirect band-gap absorption edge. These features are all similar to those in 4H-SiC.

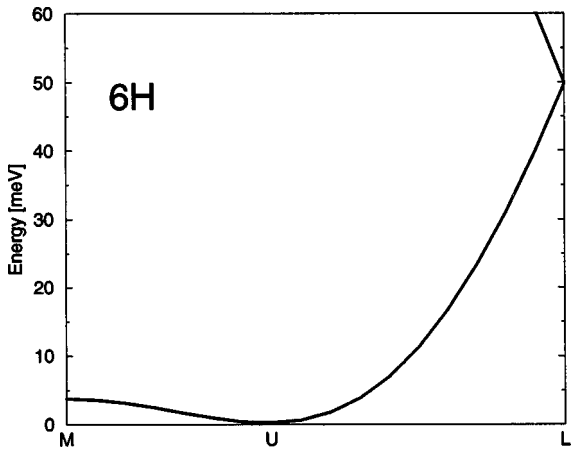

FIG. 5. Band dispersion of the lowest conduction band in 6H-SiC along the ML line; note the saddle point at M.

The main additional point of interest in 6H-SiC concerns the double-peak nature of P_1-P_2. We note that apart from a similar shift to the one that occurred in 4H-SiC, peak D_2 agrees well with P_2, while the extra peak P_1 appears to correspond more closely to p_1, i.e., to the direct band-to-band transition. Closer inspection of p_1 in Fig. 6 reveals that it is dominated by a very sharp peak corresponding to transitions at the M point rather than the minimum point along ML. This becomes clear by comparing the calculated absorption coefficients for the transitions between c_1 and c_3 for carrier concentrations chosen such that the band is filled to levels either above or below the saddle point M. Clearly, p_1

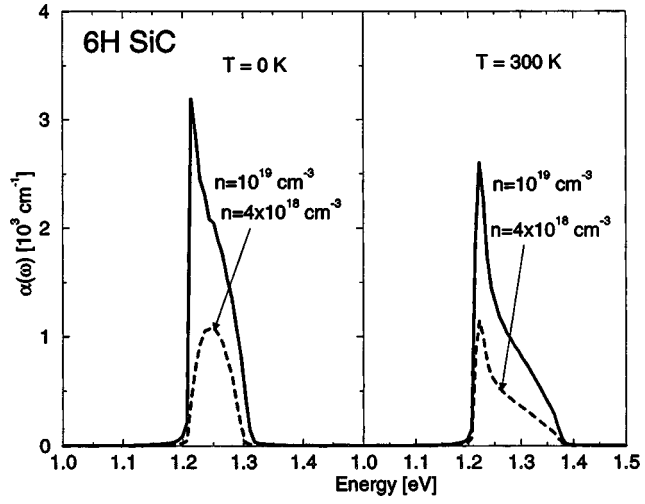

FIG. 6. Calculated $\mathbf{E}\|\mathbf{c}$ absorption spectra for 6H-SiC in the region of p_1 for two carrier concentrations and two temperatures.

is dominated by transitions from the M point if the latter is allowed to contribute. The reason for the presence of the sharp peak is that bands c_1 and c_3 are nearly parallel in the directions perpendicular to ML, in other words, they have the same transverse mass $m_\perp$. This produces a sharp one-dimensional van Hove singularity in the joint density of states. In a strict one-dimensional theory, the behavior at the singularity would be $1/\sqrt{E}$. The remnant of this in the full three-dimensional theory of the saddle point is clearly still a very sharp and strong peak.

We thus believe that the experimental feature P_1, which is characteristic of this particular polytype, is a signature of this van Hove singularity in the pure band-to-band transitions. The transitions resulting from energy levels above the M saddle point in c_1 might be expected to be more purely band-to-band-like because higher-energy bands are expected to be less mixed with the impurity band and thus to obey the $\Delta\mathbf{k}=0$ selection rule more strictly. In other words, within the range of states occupied from slightly below the conduction-band minimum to a few 10 meV above it, the nature of the states should be expected to gradually change from being more localized the farther their energy is below the band edge to more purely bandlike the farther they are above the band edge. The range of $\mathbf{k}$ space reached by the transitions for the final states would correspondingly become gradually more narrow as the initial state lies higher above the band edge.

To test the assignment of the peak P_1 experimentally, it would be interesting to observe the freeze-out of this transition at low temperatures for a sufficiently low carrier concentration. Figure 6 indeed indicates that for a carrier concentration $n=4\times10^{18}$ cm^{-3} the singularity related peak disappears at low temperature but is still present at room temperature.

In this context, it is of interest that spectra for a highly resistive (low carrier concentration) sample of n-type 6H-SiC, were reported by Stiasny and Helbig (SH).[7] Unfortunately, it does not cover the low-energy region where the effects on p_1 would be noticeable. In fact, their spectra and interpretation differ considerably from those of Biedermann.[4] On the basis of both absorption and emission spectra in the same sample, SH concluded that the absorption is associated with transitions from a deep center, not states at the conduction-band edge and associated band tail as assumed in this work. Their spectra differs from Biedermann's mainly in that the main absorption feature (P_2 for $\mathbf{E}\|\mathbf{c}$ and P_4 for $\mathbf{E}\perp\mathbf{c}$) occurs at 1.9 eV instead of 1.6 eV. Similar to Biedermann's spectrum, however, it does show peaks similar to P_3 and P_5 around 2.9 eV. Their conclusion about this being a deep center is based on the following observations: (1) the absorption spectra are nearly independent of temperature, and (2) they found an emission spectrum which is roughly similar to the absorption spectrum but shifted to lower energy by $\sim$0.2 eV. They interpreted the downward displacement as a Stokes shift in a transition involving a deep center. We disagree with this interpretation, and show that the differences between their spectra and Biedermann's can be explained within the general model adopted in the present paper.

First, we note that the luminescence spectrum can involve a variety of centers, and its interpretation can be complicated. Further, the fact that the Stokes shifts for the two emissions (at 1.9 and 2.9 eV) are nearly identical appears fortuitous. Since their n-type sample was highly resistive and contained N, it is likely that the Fermi level was pinned near the deeper N-donor level at $\sim$140 meV below the conduction band, not at the shallower level relevant for the samples we were mainly concerned with in this paper. If we interpret the features as transitions from this level to the conduction bands, this would reflect itself in a rather weak T dependence in the 10–300-K range, as was observed. So, the weak temperature dependence does not prove their interpretation.

The remaining and nontrivial issue is the 0.3-eV upward shift of the prominent peak. This cannot be explained by the roughly 0.06 eV additional binding energy. But the larger binding energy has other consequences: greater relaxations of the polarization and $\Delta\mathbf{k}=0$ selection rules. The former follows from the greater mixing of the c_1 and c_2 conduction bands into the donor level, which even may cease to be describable by effective mass theory.[16] The SH spectra in fact exhibit a significantly weaker polarization dependence than Biedermann's spectra. Within our model, the stronger localization of the donor wave function implies a larger range of $\mathbf{k}$ than used above. This tends to push the peak position to higher energy because higher bands can be reached within a larger $\mathbf{k}$ sphere. The peak position results effectively from the δk cutoff. Simultaneously, peak D_4 makes a more sizable contribution to P_2 because of the breaking of the polarization selection rules. We have verified by explicit calculations that increases by 30–50 % in δk could effectively move the peak upward by $\sim$0.3 eV. The peaks also become even broader, which is also consistent with the SH spectra. In other words, there is no need to invoke a new deep center to explain the SH data. There is only a quantitative, not a qualitative, difference resulting from the more localized nature of the deeper donor states. In addition to these responses to SH, we note that the model employed here provides quite satisfactory results for the entire set of spectra for all five polytypes for which data exist.

As far as relative intensities are concerned, we again focus only on the two prime absorption features: P_2 and P_4. Again, as in 4H, the corresponding final state DOS factors appear to be equally strong, while P_2 is at least an order of magnitude stronger than P_4. This is consistent with the fact that the matrix element squared is found to be about 20 times stronger for $c_1\rightarrow c_3$ than for $c_1\rightarrow c_4$.

One more feature remains to be explained about the 6H spectra. In samples of intermediate doping level, e.g., $n=4\times10^{18}$ cm^{-3}, the authors of Ref. 2 observed a peak for $\mathbf{E}\perp\mathbf{c}$ at about 1.1 eV. For higher concentrations, this peak is submerged under the free-carrier absorption while for carrier concentrations 5×10^{17} cm^{-3} it is absent. Our calculations provide no straightforward explanation for this feature. One might think of transitions from c_2 to c_3; however for $n=4\times10^{18}$ cm^{-3} and with band c_2 located at about 100 meV above the minimum, there is only a weak occupancy at room temperature. It is thus not easy to explain how this absorption feature can be as strong as the $c_1\rightarrow c_4$ transition, i.e., P_4 at 2 eV, as observed in Ref. 2. This would only be possible if the matrix elements for this transition are rather strong. Inspection of the matrix elements, however, reveals that the $c_2\rightarrow c_3$ transition for $\mathbf{E}\perp\mathbf{c}$ is actually weaker than the c_1

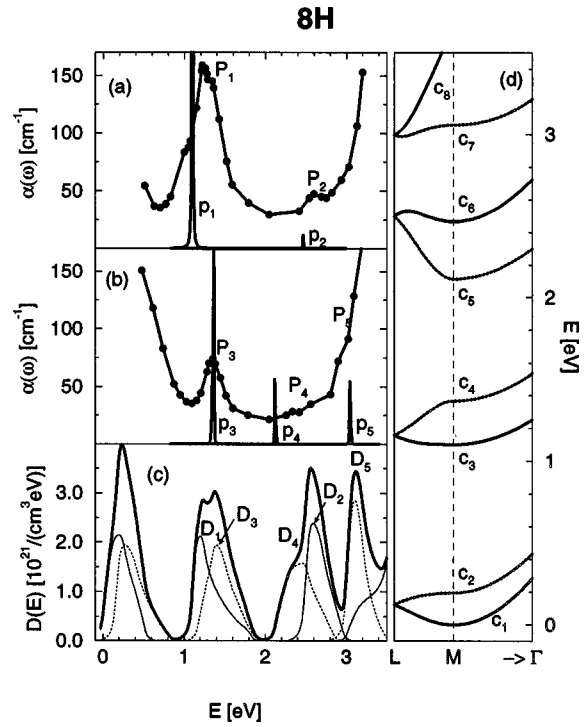

FIG. 7. Band structure and inter-conduction-band spectra in *n*-type 8H-SiC: (a) $\mathbf{E}\|\mathbf{c}$ and (b) $\mathbf{E}\perp\mathbf{c}$ experimental absorption spectra from Ref. 4 (lines connecting dots), with capitalized peak labels P_i compared to calculated spectrum in pure band-to-band limit (full line) peaks labeled by lower case p_i (assuming $n=10^{19}$ cm^{-3} and $T=300$ K). (c) Calculated density of states within $\delta k=0.1\ [2\pi/a]$ from $\mathbf{k}_{min}=M$. Thick line: total; full thin line: M_1 symmetry bands; dashed line: M_3 symmetry. (d) Energy bands: full lines correspond to M_1 symmetry, and dashed lines to M_3 symmetry at *M*.

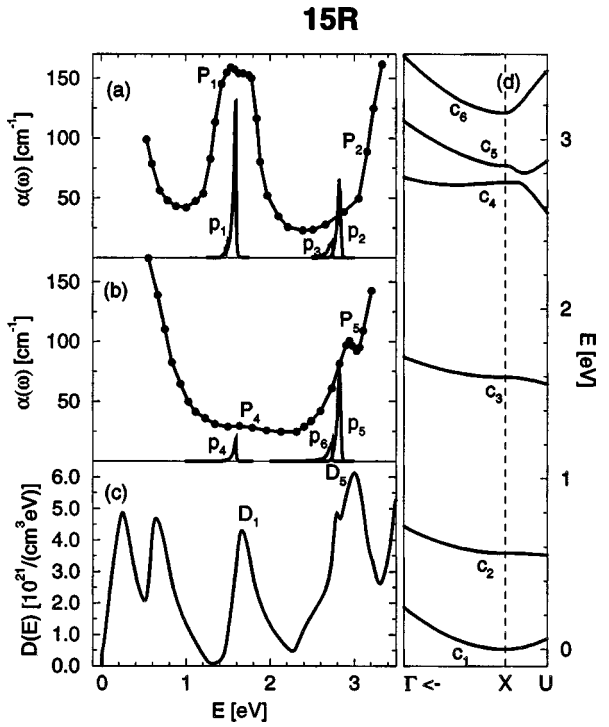

FIG. 8. Band structure and inter-conduction-band spectra in *n*-type 15-SiC: (a) $\mathbf{E}\|\mathbf{c}$ and (b) $\mathbf{E}\perp\mathbf{c}$ experimental absorption spectra from Ref. 4 (lines connecting dots) with capitalized peak labels P_i compared to calculated spectrum in pure band-to-band limit (full line) peaks labeled by lower case p_i (assuming $n=10^{19}$ cm^{-3} and $T=300$ K). (c) Calculated density of states within $\delta k=0.1\ [2\pi/a]$ from $\mathbf{k}_{min}=X$. (d) Energy bands around *X*.

$\rightarrow c_4$ transitions. Thus this explanation is not tenable. The only explanation we can presently offer is that this could be a contamination effect by the presence of higher order polytypes. As shown below, for 8H for example, transitions do occur for $\mathbf{E}\perp\mathbf{c}$ at about 1.1 eV.

D. 8H

The results for 8H are shown in Fig. 7, which is organized in the same way as the figures for 4H and 6H. In this case, we expect from the symmetry of the bands the following transitions: for $\mathbf{E}\|\mathbf{c}$, $c_1\rightarrow c_3$ at 1.1 eV and $c_1\rightarrow c_6$ at 2.5 eV, corresponding to P_1 and P_2; for $\mathbf{E}\perp\mathbf{c}$, $c_1\rightarrow c_4$ at 1.4 eV, $c_1\rightarrow c_5$ at 2.1 eV, and $c_1\rightarrow c_7$ at 3 eV, corresponding to P_3-P_5. Good agreement is observed between the experimental and the predicted transition energies for each polarization. Again, the widths of these peaks are much better described by the partial **k**-space DOS. As before, we note that D_1 is slightly lower in energy than P_1 whereas the higher D_i agree closely with the P_i and better than the pure band-to-band p_i predictions do. The peak P_1 probably contains some contributions from D_3 reflecting the partial breakdown of the polarization selection rule. This would explain both its upward shift and its asymmetric shape.

E. 15R

The conduction-band minimum in 15R occurs at the *X* point of the rhombohedral Brillouin zone. This point is folded on *M* in the appropriate hexagonal Brillouin zone (i.e., using a 15-layer unit cell parallel to the *c* axis instead of the five-layer rhombohedral unit cell). The direction *XU* shown in the right panel of Fig. 8 is nearly parallel to the **c** axis, as is shown qualitatively[29] in Fig. 9. Thus the symmetry of the bands used for the hexagonal polytypes and the selection rules based on them no longer strictly apply. However, by considering the small deviation from parallelism as a perturbation, one can infer that the selection rules retain some

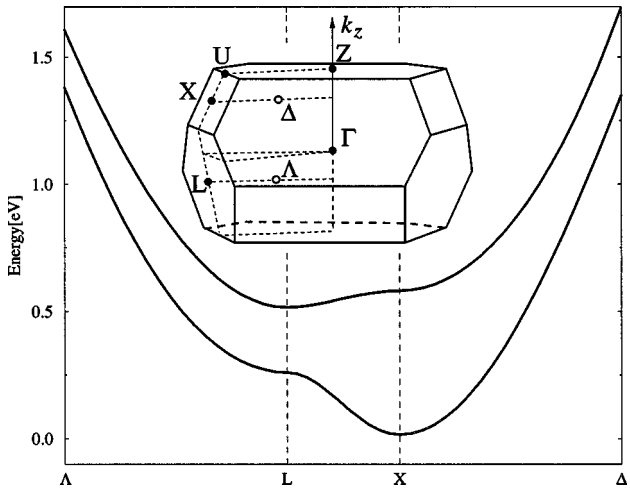

FIG. 9. Band-structure dispersion of the lowest two conduction bands in 15R-SiC. The inset shows the relevant portion of the Brillouin zone (Ref. 29).

usefulness. This is reflected in the facts that the observed P_1 peak is strongly polarized, $\mathbf{E}\|\mathbf{c}$, and that the calculated matrix elements imply that polarization preference. That the transitions to the bands c_4 and c_5 have comparable strengths in both polarizations results from the close proximity in energy of these bands and their consequent mixing. As in other polytypes, the relaxation of the $\Delta\mathbf{k}=0$ selection rule clearly provides for the major part of the differences between the observed widths and those calculated using the unperturbed bands. We note that while D_5 accounts well for the width of P_5, D_1 is somewhat narrower than P_1.

On a more detailed level, the shape of P_1 suggests a two-peaked structure analogous to the one in 6H. This suggestion is, however, not supported by the calculated D_1 and p_1. If one accepts the two-peaked structure, one might, in analogy with the situation for 6H, search for a neighboring saddle point. As seen in Fig. 9, one indeed exists at the point L. However, as that saddle point is about 0.2 eV above the minimum, it would be essentially unoccupied at room temperature and hence incapable of producing a significant peak. Another possible explanation for the low-energy peak one might consider is the fact that 15R samples frequently contain regions of 6H. An one would then expect a peak at 2 eV for $\mathbf{E}\perp\mathbf{c}$, which, however, is not clearly evident in the data, this explanation is also not too persuasive.

Finally, we note that the lower part of P_1 corresponds somewhat closer to p_1, and the higher part more closely with D_1. One would further expect D_1 to shift slightly to higher energies if we take into account its origin from impurity mixed states slightly below the band. Thus the low-energy peak of P_1 could result from more purely band-to-band-like transitions, and the higher-energy peak from the more impuritylike transitions. This explanation is in fact similar to the one we offered for 6H. In fact, one expects a gradual transition between the two regimes in all polytypes. If this is true, one would expect that the peak shape of P_1 changes with temperature and carrier concentration in all cases. It is presently not clear why this two-peak nature appears more prevalent in 15R than in 4H or 8H, or why it is more important for this particular transition than for the higher energy ones. The situation for 15R is clearly different from 6H, where the two peaks are more clearly separated in the data and where the very high intensity of peak p_1 (the maximum of the peak is $>500\ \mathrm{cm}^{-1}$) can be explained by the occurrence of occupied van Hove singularity. As implied above, further study of the line shapes of the absorption spectrum with varying temperature and carrier concentration is desirable.

IV. CONCLUSION

In this paper, we have investigated the validity of the interpretation of the 1–3-eV absorption features in fairly heavily doped *n*-type SiC polytypes in terms of transitions from the lowest conduction band to higher bands. We find that this model is in good agreement with the energy band differences calculated here using the full-potential linear muffin-tin orbital method for all the polytypes for which are presently data available, i.e., 3C, 6H, 4H, 8H, and 15R. It also satisfactorily explains the polarization dependence of the spectra in terms of selection rules and the symmetry of the bands, and even explains qualitatively the relative intensities of the main absorption features for different polarization in terms of the relative magnitudes of the matrix elements. The integrated absolute order of magnitude of these absorption features is also found to be in accord with the data for the reported order of magnitude of the carrier concentrations present in these samples. Discrepancies in the conduction-band separations are of order 0.1 eV maximum, which may in part be due to our neglect of quasiparticle corrections.

However, the fact that the widths of the features in the measured absorption spectra are about ten times wider than the calculated ones on the basis of an unperturbed band-to-band model indicates that impurity effects are important. For the carrier concentrations typical of the samples investigated, the shallow N impurities form a impurity band overlapping with the bottom of the conduction band, known as a band tail. Since the initial states are thus partially localized in nature, the vertical selection rule must be relaxed. We showed that the observed widths of the spectra can be accounted for by relaxing the $\Delta\mathbf{k}=0$ selection rule and assuming that transitions occur to final states within a certain range of $\mathbf{k}$ space of order $\delta k\approx 0.1\ [2\pi/a]$, which is approximately the range of $\mathbf{k}$ in the wave function for a shallow N donor. Nevertheless, the transitions essentially maintain the polarization behavior of the pure band-to-band model. This means that the impurity band states in question must be derived primarily from the lowest conduction band, and thus to a large extent reflect its symmetry character. The above line of argument also suggests that the higher conduction states are less affected by the presence of the impurities. As far as the initial states are concerned, one expects a gradual change from the more localized states (for which the energy is farthest below the band edge and which involve a strong breakdown of the virtual selection rule) to more purely bandlike states for states with energies higher and higher above the band edge. This would in general suggest that the peak shapes may change with carrier concentration and temperature. In particular, at lower impurity concentrations one expects a freeze-out at low temperature of the more purely band-to-band-like features, and a spectrum more dominated by impurity to band transitions. So far, this has been explored experimentally only to a limited extent because the studies that correlated the absorption features with the carrier concentrations (obtained by Hall measurements) were limited to 6H and to $\mathbf{E}\perp\mathbf{c}$. Unfortunately, the most characteristic and strongest absorption feature occurs for $\mathbf{E}\|\mathbf{c}$.

Among the spectra for the various polytypes, probably the most interesting one occurs for 6H, as it exhibits a clear two-peak feature for $\mathbf{E}\|\mathbf{c}$ in its prominent feature. We showed that this unique feature is related to the presence of a one-dimensional van Hove singularity in the joint density of states of pure interband transitions at the M point in the Brillouin zone. According to our (and other) first-principles calculations, the M point in the lowest conduction band is a saddle point, while the minima occur in six inequivalent very shallow valleys centered at a point along the ML axis. Thus a further study of the behavior of this absorption feature may provide experimental evidence for this six valley model in 6H-SiC. The alternative explanation of spectra in this energy range in a very highly resistive sample of 6H in terms of a deep center proposed by Stiasny and Helbig[7] was rejected

because their observations can be explained within the context of our present model by simply assuming a slightly more localized initial state.

A few aspects in the body of experimental data on these spectra are presently unsettled. These are the 1.1-eV feature for $\mathbf{E}\perp\mathbf{c}$ in 6H reported in only one study, and clearly identifiable only for intermediate carrier concentrations and the possible ''two-peak'' nature of the $\mathbf{E}\|\mathbf{c}$ spectrum in 15R. Neither of these observations can be understood in terms of our present slightly modified band structure model which satisfactorily explained the bulk of the experimental data available in this energy range. These questions thus warrant further experimental study.

ACKNOWLEDGMENTS

This work was supported by the National Science Foundation under Grant No. DMR-95-29376. We wish to thank W. J. Choyke for bringing the ''Biedermann'' spectra to our attention.

[1] J. A. Lely and F. A. Kröger, in *Halbleiter und Phosphore, Conference on the Physics of Semiconductors (Garmish-Partenkirchen)*, edited by Michael Schön and Heinrich Welker (Vieweg-Verlag, Braunschweig, 1956), p. 514.

[2] G. N. Violina, Yeh Liang-hsiu, and G. F. Kholuyanov, Fiz. Tverd. Tela (Leningrad) **5**, 3406 (1963) [Sov. Phys. Solid State **5**, 2500 (1964)].

[3] B. Ellis and T. S. Moss, Solid State Commun. **3**, 109 (1965).

[4] E. Biedermann, Solid State Commun. **3**, 343 (1965).

[5] L. Patrick and W. J. Choyke, Phys. Rev. **186**, 775 (1969).

[6] G. B. Dubrovskii and E. I. Radovanova, Fiz. Tverd. Tela (Leningrad) **11**, 680 (1969) [Sov. Phys. Solid State **11**, 545 (1969)].

[7] Th. Stiasny and R. Helbig, Phys. Status Solidi A **162**, 239 (1997).

[8] W. R. L. Lambrecht, in *Diamond, SiC and Nitride Wide Bandgap Semiconductors*, edited by C. H. Carter, Jr., G. Gildenblat, S. Nakamura, and R. J. Nemanich, MRS Symposia Proceedings No. 339 (Materials Research Society, Pittsburgh, 1994), p. 565.

[9] W. R. L. Lambrecht, S. Limpijumnong, and B. Segall, in *Silicon Carbide and Related Materials*, edited by S. Nakashima, H. Matsunami, S. Yoshida, and H. Harima, IOP Conf. Proc. No. 142 (Institute of Physics, Bristol, 1996), p. 263.

[10] W. R. L. Lambrecht, S. Limpijumnong, S. N. Rashkeev, and B. Segall, Phys. Status Solidi B **202**, 5-33 (1997).

[11] W. R. L. Lambrecht. S. Limpijumnong, and B. Segall, in *Silicon Carbide, III-Nitrides and Related Materials*, Proceedings of the 7th International Conference on Silicon Carbide, III-Nitrides and Related Materials, Stockholm, Sweden, September 1997, edited by G. Pensl, H. Morkoç, B. Monemar, and E. Janzen (Trans Tech, Uetikon-Zuerich, 1998), Pt. 1, pp. 271–274.

[12] N. T. Son, O. Kordina, A. O. Konstantinov, W. M. Chen, E. Sörman, B. Monemar, and E. Janzén, Appl. Phys. Lett. **65**, 3209 (1994).

[13] W. R. L. Lambrecht and B. Segall, Phys. Rev. B **52**, R2249 (1995).

[14] G. Pensl and W. J. Choyke, Physica B **185**, 264 (1993).

[15] B. Segall, S. A. Alterovitz, E. J. Haugland, and L. G. Matus, Appl. Phys. Lett. **49**, 584 (1986).

[16] A-B. Chen and P. Srichaikul, Phys. Status Solidi B **202**, 81 (1997).

[17] O. K. Andersen, O. Jepsen, and M. Šob, in *Electronic Band Structure and its Applications*, edited by M. Yussouff (Springer, Heidelberg, 1987), p. 1.

[18] W. R. L. Lambrecht, B. Segall, M. Yoganathan, W. Suttrop, R. P. Devaty, W. J. Choyke, J. A. Edmond, J. A. Powell, and M. Alouani, Phys. Rev. B **50**, 10 722 (1994).

[19] S. N. Rashkeev, W. R. L. Lambrecht, and B. Segall, Phys. Rev. B **57**, 9705 (1998).

[20] S. N. Rashkeev, W. R. L. Lambrecht, and B. Segall, Phys. Rev. B **57**, 3905 (1998).

[21] M. Methfessel, Phys. Rev. B **38**, 1537 (1988).

[22] L. Hedin and B. I. Lundqvist, J. Phys. C **4**, 2064 (1971).

[23] P. Hohenberg and W. Kohn, Phys. Rev. **136**, B864 (1964); W. Kohn and L. J. Sham, *ibid.* **140**, A1133 (1965).

[24] M. Rohlfing, P. Krüger, and J. Pollmann, Phys. Rev. B **48**, 17 791 (1993).

[25] W. H. Backes, P. A. Bobbert, and W. van Haeringen, Phys. Rev. B **51**, 4950 (1994).

[26] B. Wenzien, P. Käckell, F. Bechstedt, and G. Cappellini, Phys. Rev. B **52**, 10 897 (1995).

[27] W. R. L. Lambrecht, B. Segall, M. Methfessel, and M. van Schilfgaarde, Phys. Rev. B **44**, 3685 (1991).

[28] É. I. Rashba, Fiz. Tverd. Tela (Leningrad) **1**, 407 (1959) [Sov. Phys. Solid State **1**, 368 (1959)].

[29] Qualitatively, the *c* direction is not drawn to scale with respect to the in-plane directions so as to facilitate labeling. The actual *c* axis should be shortened by 60%.